Assessing the potential of polarimetric decomposition of Sentinel-1 SAR for the estimation of mangrove forest biomass

Giusti Ghivarry[1], Erico Kutchartt[1,2], Francesco Pirotti[1,3]

[1]Department of Land, Environment, Agriculture and Forestry (TESAF), University of Padova, Legnaro, Italy – giusti.ghivarry@studenti.unipd.it, erico.kutchartt@unipd.it, francesco.pirotti@unipd.it
[2]Forest Science and Technology Centre of Catalonia (CTFC). Carretera de Sant Llorenç de Morunys, Km 2, 25280 Solsona, Spain - erico.kutchartt@ctfc.cat
[3]Interdepartmental Research Center of Geomatics (CIRGEO), University of Padova, Legnaro, Italy

Keywords: H-α dual pol decomposition, synthetic aperture radar, dual polarization, GEDI L4A, mangrove biomass

Abstract:

Mangrove forests provide ecosystem services that can support the welfare of local communities. Therefore, promoting their conservation not only protects their environmental functions but also optimizes their economic potential. Remote sensing approaches, particularly active systems such as synthetic aperture radar (SAR), have emerged as a valuable tool for monitoring forest ecosystems. These systems can capture Earth's surface features regardless of atmospheric conditions. However, the backscatter approach becomes unreliable when the AGBD reaches a certain point. This leads to incomplete information being obtained as the reflected signal becomes too strong and overloads the receiver. Therefore, this study explores the potential of polarimetric decomposition as an option to traditional backscatter approaches. Decomposed polarimetric parameters from Sentinel-1 were used for biomass estimation in mangrove forests in West Kalimantan Province. Specifically, in Kubu Raya and North Kaong districts (Indonesia) for the year 2020. The decomposed polarimetric parameters of Entropy, Anisotropy, and Alpha Angle obtained from the H/A/α decomposition integrated with backscattering parameters were used as dependent variables, which were varied following the parameter usage scenarios (both individual and grouped). Meanwhile, GEDI data were used to train the prediction model instead of observational data. The predictive ability of the model using only SAR-derived explanatory variables resulted in an RMSE of about 45 Mg/ha and an R-squared of about 0.2.

1. Introduction

Mangrove forests are one of the most important ecosystems for surrounding communities because they can provide interrelated tangible and intangible environmental services. These included not only cultural services in the form of ecotourism and cultural heritage (Bimrah et al., 2022) but also protective functions against waves and tides (Marois and Mitsch, 2015). Additionally, their restoration and conservation can generate revenue through carbon markets due to their ability to store blue carbon (Van Zanten et al., 2021). The conservation of blue carbon is appealing as it offers additional benefits such as fish habitat protection and water filtration (Dalimunthe et al., 2022). Recognizing these extensive benefits, Indonesia has been actively involved in mangrove forest restoration, with a national plan to rehabilitate 3.49 million hectares by 2045 (Sasmito et al., 2023). Furthermore, the Peat and Mangrove Restoration Agency (BRGM) was established in 2020 with a more ambitious goal to rehabilitate 600,000 hectares by 2024 (Rahman et al., 2024).

Understanding the state of mangrove forests is crucial for effective conservation strategies. This requires accurate and up-to-date data on their location and health. Remote sensing provides a powerful tool for efficiently mapping these ecosystems (Kuenzer et al., 2011). And recent studies explored the use of active systems (such as SAR) with promising results due to their sensitivity to structural features (Pham et al., 2019). However, the reflected signal from SAR can sometimes be too powerful, leading to data loss, prompting the exploration of alternative approaches (Joshi et al., 2017).

The strength of SAR backscatter depends on intrinsic characteristics like SAR wavelength and polarization, as well as surface properties including water content and material roughness. Additionally, topography significantly affects the incidence angle of the SAR signal and must be considered. For instance, Pirotti et al. (2023) demonstrated that canopies have a strong absorption of the backscatter signal, thus resulting in weaker backscatter, but when the canopies are completely wet, the backscatter is up to 2 dB stronger. This correlation is lost after fire events, likely due to thin biomass being burned away and thicker branches being left as reflectors.

One promising approach is the polarimetric decomposition method. Several studies have been applied to quad-polarization and dual-polarization SAR data. Studies by Zeng et al. (2022) and Liu et al. (2022) evaluated the polarimetric decomposition for AGB estimation on quad- polarization data of Gaofen-3, RADARSAT-2, and ALOS-2/PALSAR-2. The evaluation resulted in improved AGB estimation accuracy compared to traditional backscattering coefficients. Particularly, the Yamaguchi decomposition has shown the highest correlation with the AGB compared to other decomposition methods (Liu et al., 2022). Nevertheless, parameters derived from other decomposition methods, such as Pauli decomposition and H/A/α, were also identified (Sinha, 2022). Particularly on ALOS/PALSAR data over tropical deciduous forests, which showed moderate correlation.

On the other hand, the parameters of the H/A/α decomposition method on Sentinel-1 Imagery have been widely studied for various applications. The study by Kiyohara and Sano (2023) utilized Entropy and Alpha Angle for forest classification in the

Amazon with support vector machine (SVM), resulting in good accuracy for distinguishing secondary forest. However, studies by Zhou et al. (2021) and Fatnassi et al. (2023) showed limitations in dense forests (multiple reflections in mangroves) and for specific class distinctions (forest vs. other). Another study by Ghazali and WIkantika (2021) utilized the H/A/α decomposition with other parameters for mangrove species classification, which resulted in fairly good accuracy (up to 65%).

This research focusses on the application of Sentinel-1 SAR data to predict mangrove forest biomass in West Kalimantan in 2020. Instead of relying solely on the signal amplitude, parameters derived from the manner of wave propagation (polarimetric decomposition) are incorporated into the model. This study aims to achieve three main objectives: 1) Build a model that incorporates backscattering and these scattering mechanism parameters, along with biomass data from GEDI, to estimate biomass density. 2) Assess how well these parameters capture biomass variations compared to backscattering alone. 3) To compare the accuracy of their new model with existing methods used to estimate mangrove biomass.

2. Study Area

Indonesia is one of the countries with extensive mangrove ecosystems on its large islands (Kusmana, 2014). According to the Global Mangrove Watch (GMW), it is calculated that Indonesia's mangrove forest area reached ~2.95 million ha in 2020 (Bunting et al., 2022). Meanwhile, the Indonesian Ministry of Environment and Forestry (IMEF) estimated the mangrove forest area at ~3.36 million ha in 2021. It included existing protected, conservation, and production forests, with the potential for further restoration efforts in identified potential mangrove areas. This biodiversity-rich area has 240 species, with most found on Java Island, and 48 species of true mangroves such as *Rhizophora spp.*, *Avicennia spp.*, and *Sonneratia spp*. (Rahman et al., 2024).

The development of the aboveground biomass estimation model was carried out in mangrove forest areas in the western part of West Kalimantan province, precisely in Kubu Raya Regency and Kubu Raya District. Based on calculations from GMW (Bunting et al., 2022), the mangrove forest used in this study has an area of ~90,000 ha. This mangrove forest covers the coastline of Kubu Raya and North Kayong districts. This includes the mangrove forest on Padangtikar Island in Kubu Raya Regency and the mangrove forest on Maya Island in North Kayong Regency. The intended study locations can be seen in Figure 1.

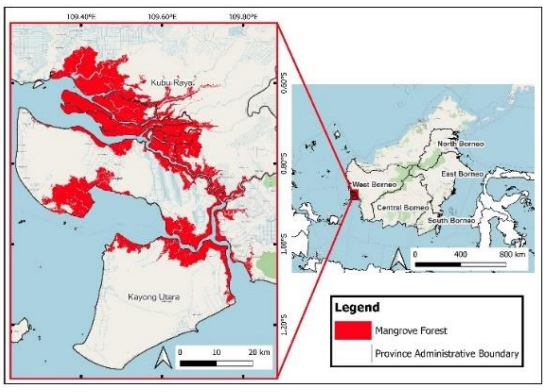

Figure 1: A map of the study site, located in Kubu Raya District and Kubu Raya Regency, West Kalimantan Province, is marked with a red box.

3. Materials and Methods

3.1 Materials

In this study, mangrove forest biomass in Kubu Raya and Kayong Utara regencies, West Kalimantan, was predicted with remote sensing data. The remote sensing data used are Sentinel-1 Level-1 synthetic aperture radar (SAR) images with single look complex (SLC) and ground range detected (GRD) formats. The SLC format file was obtained from the tilt and azimuth range at the time of data acquisition (ESA, 2024a). While the GRD format was obtained by applying detection, multi-looking, and projection on the ground surface area using an earth model, resulting in an image with square-shaped pixels and relatively even resolution across the image due to multi-looking processing that only represents signal strength (ESA, 2024b). To enrich the data sources for estimation purposes, several images acquired during 2020 have been used. Sentinel-1 SAR images have advantages in terms of their ability to penetrate clouds and vegetation, so they can be used to obtain mangrove forest biomass information (Chen et al., 2017).

Samples for model training and validation were obtained from the Global Ecosystem Dynamic Investigation (GEDI) Level 4A (L4A) Raster Aboveground Biomass Density (AGBD) Version 2.1 (Google Earth Engine Developer, 2024). This laser-based data was able to show the three-dimensional structure of the vegetation (Kutchartt et al., 2022), which can be further processed to obtain biomass information. In addition, a mangrove forest boundary map from GMW proposed by Bunting et al. (2018) was utilized, which aimed to determine mangrove and non-mangrove forest boundaries. This map had high accuracy, so it could be used to ensure that the training and validation samples were in mangrove forest areas. Additionally, other estimation models, such as the Climate Change Initiative (CCI) Biomass Map by ESA (Santoro and Cartus, 2023), were also used for comparison with the resulting estimation model. A brief description of the data used and the purpose of using the data can be seen in Table 1 below.

Source	Level	Pixel Size (m)	Description
Sentinel-1 L1 SAR	SLC	15	Polarimetric Decomposition parameter extraction
Sentinel-1 L1 SAR	GRD	10	Backscatter Parameter extraction
GEDI	L4A AGBD	25	Lidar base AGBD information
GMW Mangrove Extent	Yearly Mosaic	10	Mangrove forest extent
CCI Biomass Map	Yearly Mosaic	100	Global-scale AGB map for comparison

Table 1: Recapitulation of the utilized geo-spatial data.

3.2 Methods

The workflow conducted in this study was divided into three interconnected stages, namely data pre-processing, model building, and model performance assessment and validation. The

pre-processing stage was carried out with the objective of tidying the data so that it can represent accurate and precise information. This stage also includes preprocessing satellite images to obtain SAR parameters, as well as processing and choosing GEDI data (Dubayah et al. 2020) to obtain training and validation samples.

The H/A/α decomposition method that has been modified by Cloude (2007) and Ji and Wu (2015) to be applicable to dual polarization data has been employed to obtain the decomposed polarimetric parameters. H/A/α decomposition, also known as Cloude-Pottier Decomposition, is an eigenvalue/eigenvector-based method that decomposes the cooccurrence or covariance matrix to obtain Entropy (H), Anisotropy (A), and Alpha Angle (α) (Cloude and Pottier, 1997). According to Pottier (2017), Entropy is a measure of randomness or disorder in a scattering system that describes the scattering process. Next to Entropy, Anisotropy is a parameter that provides details about the specific distribution in the scattering system. Finally, the Alpha Angle parameter acts as an indicator, indicating the type of scattering mechanism at play.

The next step is to build a model to predict biomass in the mangrove ecosystem. In this process, the development of the prediction model uses the H2O AutoML supervised machine learning algorithm developed by H2O.ai (LeDell and Poirier, 2020), where SAR parameters and biomass information are derived from GEDI and are used as dependent and independent variables. To determine the ability of decomposed polarimetric parameters in the estimation process, several scenarios were made based on the number of variables used in the modelling, which are shown in Table 2. Additionally, to accommodate the horizontal accuracy of GEDI data, a new dataset based on the resampling and aggregation process into pixels with coarser sizes was conducted (Shendryk, 2022), whose details are shown in Table 3.

The last step was to carry out a validation process, computing accuracy metrics, where the developed prediction model was evaluated for its predictive ability with respect to its statistical metrics. The metrics used were the coefficient of determination (R^2), root mean squared error (RMSE), mean absolute error (MAE), and mean squared error (MSE). Additionally, the biomass prediction value of the developed model was compared with the CCI ESA prediction model.

Scenarios	Parameters
1	VV Topography Uncorrected, VH Topography Uncorrected
2	VV Topography Corrected, VH Topography Corrected
3	Entropy, Anisotropy, Alpha Angle
4	VV Topography Uncorrected, VH Topography Uncorrected, Entropy, Anisotropy, Alpha Angle
5	VV Topography Corrected, VH Topography Corrected, Entropy, Anisotropy, Alpha Angle

Table 2: Scenarios to generate a mangrove forest biomass prediction model, including the parameters used for each scenario.

No	Configuration Description
1	Dataset resampled and aggregated pixel values with the median method and a 25-meter grid size.
2	Dataset resampled and aggregated pixel values with the median method and a 100-meter grid size.
3	Dataset resampled and aggregated pixel values with the mean method and a 25-meter grid size.
4	Dataset resampled and aggregated pixel values with the mean method and a 100-meter grid size.

Table 3: Configuration of the dataset used to train the prediction model.

4. Results and Discussions

4.1 Mangrove forest biomass estimation model performance

4.1.1 Statistic metric-based assessment

This study investigated the capability of decomposed polarimetric parameters when integrated to predict mangrove forest biomass. For this purpose, parameter usage scenarios (Table 3) were introduced into the training process of the mangrove forest biomass prediction model. In addition, the dataset used to train the model was also set up following the configuration described in Table 4 to see the effect of the configuration of the dataset on the modelling results. From such an arrangement, a trained model was obtained for each parameter usage scenario based on the variation of dataset configurations, whose summary statistical metrics are represented in Figure 2 as follows:

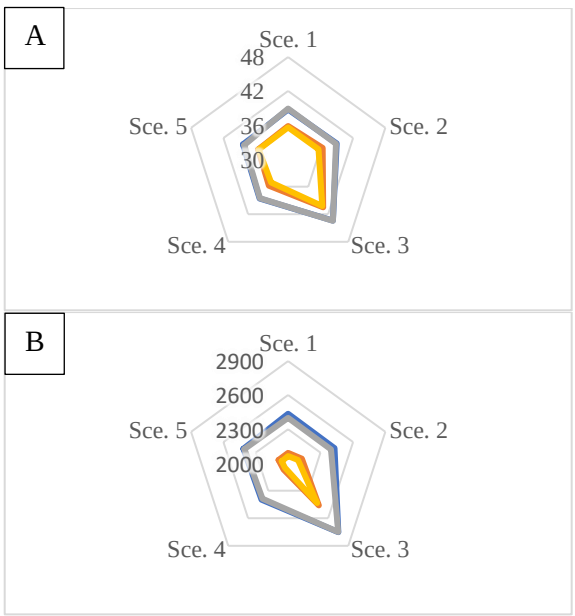

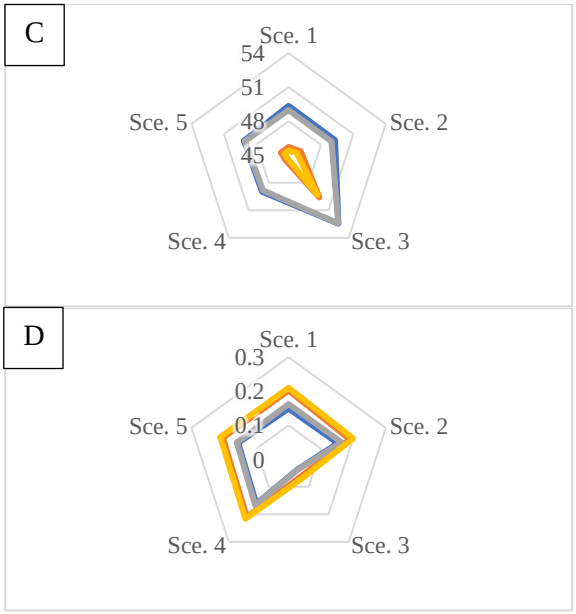

Figure 2: Graph representation of the statistical metrics of the trained model for each scenario grouped by dataset configuration for model training, where (A) MAE, (B) MSE, (C) RMSE, and (D) R^2.

The incorporation of all parameters during model training resulted in marginally better results, regardless of the dataset. This is consistent with prior research by Zeng et al. (2022) and Dave et al. (2023), who showed that using phase information from decomposed polarimetric parameters improves prediction despite employing different methods and materials. However, backscatter with uncorrected topography resulted in even better results, indicating that topography correction can be counterproductive for mangrove biomass prediction. While these decomposed parameters improved model performance, they exhibited a weak correlation with biomass itself, as observed in de Jesus et al. (2023). This highlights the limitations of using single-wavelength SAR data (C-band) for biomass prediction, as it restricts the range of detectable forest components (Santoro and Cartus, 2023).

On the other hand, finer grid detail in the dataset resulted in lower prediction accuracy, suggesting that including generalized information from coarser grids is preferable when detailed physical data is absent (Figure 2). This aligns with the finding that the grouping method has minimal influence, though a mean grouping method results in slightly better results.

4.1.2 Shift in predicted biomass value range after polarimetric decomposition parameter inclusion into the model

The impact of decomposed polarimetric parameters on the range of predicted biomass values in mangrove biomass prediction models has also been investigated, and the distribution is depicted in Figure 3.

The inclusion of decomposed polarimetric parameters in the prediction models resulted in mixed effects on the range of predicted biomass values. While the maximum predicted biomass generally increased with these parameters, the effect was not consistent across all dataset configurations, except configuration one. Interestingly, some models with configuration three even predicted negative biomass values when both corrected and uncorrected backscatter data were combined with decomposed parameters.

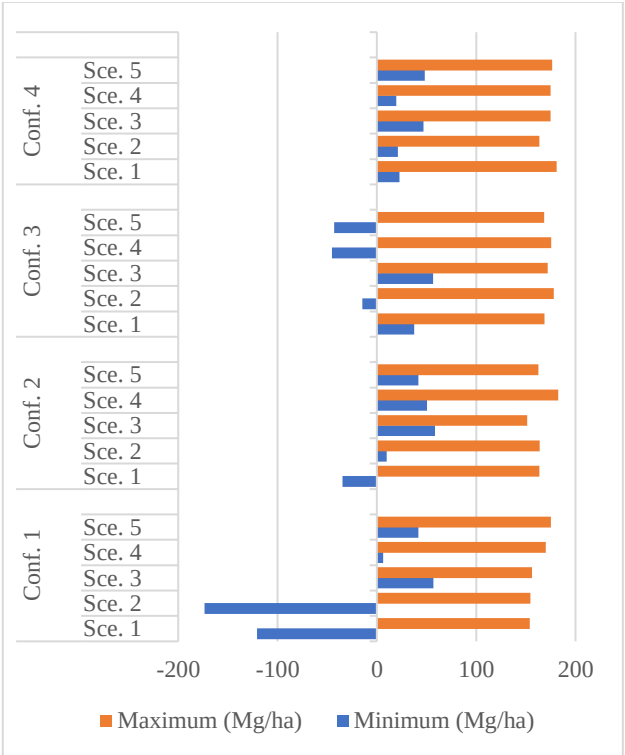

Figure 3: Predicted biomass value range (Mg/ha) of each scenario is grouped by dataset configuration for model training.

Introducing decomposed polarimetric parameters can significantly alter the minimum and maximum predicted biomass values. The heatmap in Figure 4 visualizes this effect, where green represents the highest predicted values and the opposite for the minimum. Scenarios one and two used backscatter parameters only (with and without topography correction), while scenarios four and five incorporated decomposed parameters with both corrected and uncorrected backscatter, respectively. The impact of decomposed parameters is evident by comparing the range of values between scenarios one and four and two and five.

	Sce. 1	Sce. 2	Sce. 3	Sce. 4	Sce. 5
Maximum Range (Mg/ha)					
Conf. 1	154.0	154.7	156.1	170.2	175.3
Conf. 2	163.5	164.0	151.4	182.7	162.7
Conf. 3	168.6	178.2	171.9	175.6	168.5
Conf. 4	181.1	163.5	174.8	174.8	176.4
Minimum Range (Mg/ha)					
Conf. 1	-120.5	-173.6	57.0	6.3	41.8
Conf. 2	-34.6	10.0	58.7	50.4	41.8
Conf. 3	37.6	-14.6	56.8	-45.2	-43.1
Conf. 4	22.9	21.3	47.0	19.4	48.3

Figure 4: The maximum and minimum range of predicted models (in Mg/ha).

The addition of decomposed polarimetric parameters also did not consistently reduce the minimum range of predicted biomass values. Out of all the combinations of scenarios and dataset configurations, only scenario four that used the dataset with

configuration four experienced a decrease in the minimum value range. Scenarios four and five that used the datasets with configurations one and three also technically decreased the minimum value, but the predicted biomass was at a negative value. The exception was seen in scenario four, which used the dataset with configuration one. In which the minimum range obtained was the lowest when compared to the other models, despite initially being recorded as a negative value.

4.2 Comparative assessment against other product

The range of the difference in biomass values provides an insight into the relative predicted biomass values between the developed prediction model and the CCI prediction model. This was done by subtracting the predicted values of the developed models from ESA's CCI prediction model. Figure 5 represents the range with different colours. Where the green colour represents the shortest range and the red colour represents the opposite. While Figure 6 illustrates the minimum and maximum limits of this value difference. Negative minimum values indicate that the predicted biomass in the developed model is lower than in the model from CCI, and positive values indicate the opposite condition.

	Sce. 1	Sce. 2	Sce. 3	Sce. 4	Sce. 5
Conf. 1	328.8	329.5	309.3	341.7	325.2
Conf. 2	336.7	320.5	293.4	342.2	327.6
Conf. 3	320.3	322.4	310.7	328.6	329.5
Conf. 4	357.5	330.1	304.4	337.8	336.3

Figure 5: The range of the difference (in Mg/ha) between the developed prediction models and the biomass model from CCI by ESA.

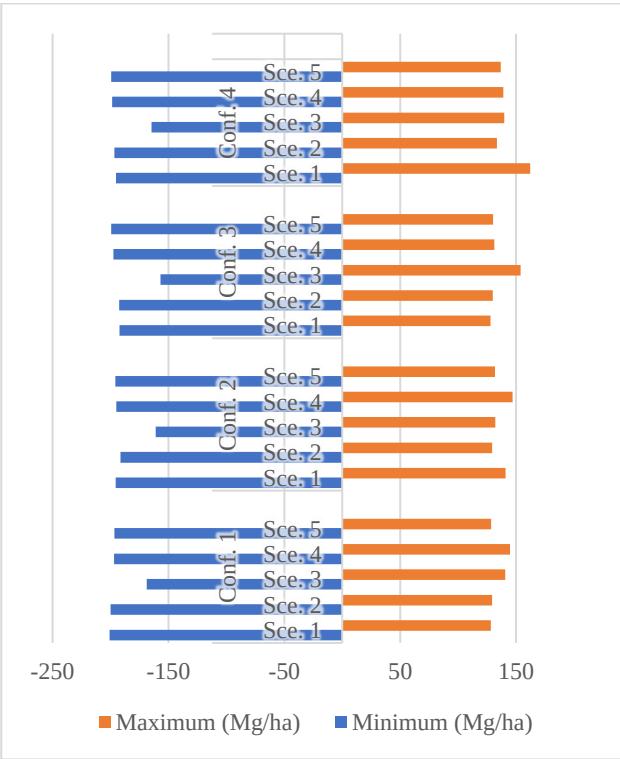

Figure 6: The range difference in predicted biomass between the developed model and ESA's CCI biomass model.

It is worth noting that the scale at which this method can be applied is regional and can complement more local biomass estimations, such as those from aerial lidar both at single-tree level (Pirotti et al., 2017) or other methods that use higher-resolution optical imagery to address forest-related matters such as forest health (Dalponte et al., 2023) or climate-change impacts (Kanan et al., 2023).

Including decomposed polarimetric parameters in the prediction models resulted in an inconsistent pattern when comparing predicted biomass values to ESA's CCI model. While some scenarios, particularly those using the dataset with configuration four, showed a reduction in the difference between the models' predictions, others exhibited an increase, especially for the dataset with configuration one. This suggests that these parameters may not significantly improve the model's ability to align with the CCI model's predictions.

Adding the decomposed polarimetric parameter to the mangrove biomass prediction also did not consistently reduce or increase the minimum range of the difference in predicted biomass between the two models. Out of the four configurations, only the models from the dataset with configuration one demonstrated a reduction in the minimum range after the decomposed polarimetric parameter was added. Indicating that with the addition of the decomposed polarimetric parameter to the prediction process, the minimum value of the predicted biomass became closer relative to the CCI biomass model.

5. Conclusion

This study investigated the influence of decomposed polarimetric parameters derived from Sentinel-1 SAR images on predicting mangrove forest biomass. GEDI biomass data served as the reference, while SAR data acted as explanatory variables. Different parameter usage scenarios were explored, incorporating backscatter and decomposed polarimetric parameters individually and together. To address the horizontal accuracy of GEDI data, a new dataset was generated by resampling and aggregating the input data onto a coarser grid. This dataset was then used for mangrove biomass modelling.

Our results found that combining decomposed polarimetric parameters with backscattering improves model performance, which is in line with previous studies. The best models used backscattering with uncorrected topography and average clustering on coarser grids, while models that used only decomposed parameters performed poorly, indicating limited standalone effectiveness. Despite the improvements, model performance was limited by the dual-polarization Sentinel-1 data, which provided less phase information than the four-polarization data. In addition, the model also generally predicted lower biomass values than the ESA CCI model, especially at higher resolutions, due to the inherent limitations of GEDI data and the biophysical complexity of mangroves.

References

Bimrah, K., Dasgupta, R., Saizen, I., 2022. Cultural Ecosystem Services of Mangroves: A Review of Models and Methods, in: *Assessing, Mapping and Modelling of Mangrove Ecosystem Services in the Asia-Pacific Region*. Springer, Singapore, pp. 239–250. https://doi.org/10.1007/978-981-19-2738-6_13

Bunting, P., Rosenqvist, A., Hilarides, L., Lucas, R.M., Thomas, N., Tadono, T., Worthington, T.A., Spalding, M., Murray, N.J., Rebelo, L.-M., 2022. Global Mangrove Extent Change 1996–

2020: Global Mangrove Watch Version 3.0. *Remote Sensing*, *14*(15), Article 15. https://doi.org/10.3390/rs14153657

Bunting, P., Rosenqvist, A., Lucas, R.M., Rebelo, L.-M., Hilarides, L., Thomas, N., Hardy, A., Itoh, T., Shimada, M., Finlayson, C.M., 2018. The Global Mangrove Watch—A New 2010 Global Baseline of Mangrove Extent. *Remote Sens. 10, 1669*. https://doi.org/10.3390/rs10101669

Chen, B., Xiao, X., Li, X., Pan, L., Doughty, R., Ma, J., Dong, J., Qin, Y., Zhao, B., Wu, Z., Sun, R., Lan, G., Xie, G., Clinton, N., Giri, C., 2017. A mangrove forest map of China in 2015: Analysis of time series Landsat 7/8 and Sentinel-1A imagery in Google Earth Engine cloud computing platform. *ISPRS J. Photogramm. Remote Sens. 131, 104–120.* https://doi.org/10.1016/j.isprsjprs.2017.07.011

Cloude, S., 2007. *The Dual Polarization Entropy/Alpha Decomposition: A PALSAR Case Study 644, 2*.

Cloude, S.R., Pottier, E., 1997. An entropy based classification scheme for land applications of polarimetric SAR. *IEEE Trans. Geosci. Remote Sens. 35, 68–78.* https://doi.org/10.1109/36.551935

Dalimunthe, S.A., Putri, I.A.P., Prasojo, A.P.S., 2022. Depicting Mangrove’s Potential as Blue Carbon Champion in Indonesia, in: Dasgupta, R., Hashimoto, S., Saito, O. (Eds.), *Assessing, Mapping and Modelling of Mangrove Ecosystem Services in the Asia-Pacific Region. Springer Nature, Singapore, pp. 167–181*. https://doi.org/10.1007/978-981-19-2738-6_9

Dalponte, M., Cetto, R., Marinelli, D., Andreatta, D., Salvadori, C., Pirotti, F., Frizzera, L., Gianelle, D., 2023. Spectral separability of bark beetle infestation stages: A single-tree time-series analysis using Planet imagery. *Ecol. Indic. 153.* https://doi.org/10.1016/j.ecolind.2023.110349

ESA, 2024a. Single Look Complex - Sentinel-1 SAR Technical Guide - Sentinel Online [WWW Document]. Sentin. Online. URL https://copernicus.eu/technical-guides/sentinel-1-sar/products-algorithms/level-1-algorithms/single-look-complex (accessed 3.17.24).

ESA, 2024b. Ground Range Detected - Sentinel-1 SAR Technical Guide - Sentinel Online [WWW Document]. Sentin. Online. URL https://copernicus.eu/technical-guides/sentinel-1-sar/products-algorithms/level-1-algorithms/ground-range-detected (accessed 3.17.24).

Fatnassi, S., Yahia, M., Ali, T., Mortula, M., 2023. Polarimetric SAR Characterization of Mangrove Forest Environment in the United Arab Emirates (UAE). *Int. J. Adv. Comput. Sci. Appl. IJACSA 14.* https://doi.org/10.14569/IJACSA.2023.0140380

Ghazali, M.F., WIkantika, K., 2021. Pre-assessment of the Potential of Dual Polarization of Sentinel 1 Data for Mapping the Mangrove Tree Species Distribution in South Bali, Indonesia, in: *2021 7th Asia-Pacific Conference on Synthetic Aperture Radar (APSAR). Presented at the 2021 7th Asia-Pacific Conference on Synthetic Aperture Radar (APSAR), pp. 1–6.* https://doi.org/10.1109/APSAR52370.2021.9688441

Google Earth Engine Developer, 2024. GEDI L4A Raster Aboveground Biomass Density, Version 2.1 | Earth Engine Data Catalog [WWW Document]. Google Dev. URL https://developers.google.com/earth-engine/datasets/catalog/LARSE_GEDI_GEDI04_A_002_MONTHLY (accessed 3.5.24).

Jesus, J.B. de, Kuplich, T.M., Barreto, Í.D. de C., Gama, D.C., 2023. Dual polarimetric decomposition in Sentinel-1 images to estimate aboveground biomass of arboreal caatinga. *Remote Sens. Appl. Soc. Environ. 29, 100897.* https://doi.org/10.1016/j.rsase.2022.100897

Ji, K., Wu, Y., 2015. Scattering Mechanism Extraction by a Modified Cloude-Pottier Decomposition for Dual Polarization SAR. *Remote Sens. 7, 7447–7470.* https://doi.org/10.3390/rs70607447

Joshi, N., Mitchard, E.T.A., Brolly, M., Schumacher, J., Fernández-Landa, A., Johannsen, V.K., Marchamalo, M., Fensholt, R., 2017. Understanding ‘saturation’ of radar signals over forests. *Sci. Rep. 7, 3505*. https://doi.org/10.1038/s41598-017-03469-3

Kanan, A.H., Pirotti, F., Masiero, M., Rahman, M.M., 2023. Mapping inundation from sea level rise and its interaction with land cover in the Sundarbans mangrove forest. *Clim. Change 176, 104.* https://doi.org/10.1007/s10584-023-03574-5

Kiyohara, B.H., Sano, E.E., 2023. Evaluation of polarimetric data and texture attributes in SAR images to discriminate secondary forest in an area of amazon rainforest. *Ciênc. Florest. 33, e71235*. https://doi.org/10.5902/1980509871235

Kuenzer, C., Bluemel, A., Gebhardt, S., Quoc, T.V., Dech, S., 2011. *Remote Sensing of Mangrove Ecosystems: A Review. Remote Sens. 3, 878–928*. https://doi.org/10.3390/rs3050878

Kusmana, C., 2014. Distribution and Current Status of Mangrove Forests in Indonesia, in: *Mangrove Ecosystems of Asia. Springer, New York, NY, pp. 37–60*. https://doi.org/10.1007/978-1-4614-8582-7_3

Kutchartt, E., Pedron, M., Pirotti, F., 2022. Assessment of canopy and ground height accuracy from GEDI LIDAR over steep mountain areas. ISPRS *Ann. Photogramm. Remote Sens. Spat. Inf. Sci. V-3–2022, 431–438.* https://doi.org/10.5194/isprs-annals-V-3-2022-431-2022

LeDell, E., Poirier, S., 2020. H2O AutoML: Scalable Automatic Machine Learning.

Liu, Z., Michel, O.O., Wu, G., Mao, Y., Hu, Y., Fan, W., 2022. The Potential of Fully Polarized ALOS-2 Data for Estimating Forest Above-Ground Biomass. *Remote Sens. 14, 669.* https://doi.org/10.3390/rs14030669

Marois, D.E., Mitsch, W.J., 2015. Coastal protection from tsunamis and cyclones provided by mangrove wetlands – a review. *Int. J. Biodivers. Sci. Ecosyst. Serv. Manag. 11, 71–83.* https://doi.org/10.1080/21513732.2014.997292

Pham, T.D., Yokoya, N., Bui, D.T., Yoshino, K., Friess, D.A., 2019. Remote Sensing Approaches for Monitoring Mangrove Species, Structure, and Biomass: Opportunities and Challenges. *Remote Sens. 11, 230*. https://doi.org/10.3390/rs11030230

Pirotti, F., Adedipe, O., Leblon, B., 2023. Sentinel-1 Response to Canopy Moisture in Mediterranean Forests before and after Fire Events. *Remote Sens. 15, 823.* https://doi.org/10.3390/rs15030823

Pirotti, F., Kobal, M., Roussel, J.R., 2017. A Comparison of Tree Segmentation Methods Using Very High Density Airborne Laser Scanner Data. *Int. Arch. Photogramm. Remote Sens. Spat. Inf. Sci. XLII-2/W7, 285–290.* https://doi.org/10.5194/isprs-archives-XLII-2-W7-285-2017

Pottier, J.-S.L., Eric, 2017. *Polarimetric Radar Imaging: From Basics to Applications*. CRC Press, Boca Raton. https://doi.org/10.1201/9781420054989

Rahman, Lokollo, F.F., Manuputty, G.D., Hukubun, R.D., Krisye, Maryono, Wawo, M., Wardiatno, Y., 2024. A review on the biodiversity and conservation of mangrove ecosystems in Indonesia. *Biodivers. Conserv. 33, 875–903.* https://doi.org/10.1007/s10531-023-02767-9

Rucha B. Dave, Koushik Saha, Amit Kushwaha, Manisha Vithalpura, Nidhin P., Abishek Murugesan, 2023. Analysing the potential of polarimetric decomposition parameters of Sentinel–1 dual-pol SAR data for estimation of rice crop biophysical parameters. *J. Agrometeorol. 25.* https://doi.org/10.54386/jam.v25i1.2039

Santoro, M., Cartus, O., 2023. ESA Biomass Climate Change Initiative (Biomass_cci): Global datasets of forest above-ground biomass for the years 2010, 2017, 2018, 2019 and 2020, v4. https://doi.org/10.5285/AF60720C1E404A9E9D2C145D2B2EAD4E

Sasmito, S.D., Basyuni, M., Kridalaksana, A., Saragi-Sasmito, M.F., Lovelock, C.E., Murdiyarso, D., 2023. Challenges and opportunities for achieving Sustainable Development Goals through restoration of Indonesia’s mangroves. *Nat. Ecol. Evol. 7, 62–70.* https://doi.org/10.1038/s41559-022-01926-5

Shendryk, Y., 2022. Fusing GEDI with earth observation data for large area aboveground biomass mapping. *Int. J. Appl. Earth Obs. Geoinformation 115, 103108.* https://doi.org/10.1016/j.jag.2022.103108

Sinha, S., 2022. H/A/α Polarimetric Decomposition Of Dual Polarized Alos Palsar For Efficient Land Feature Detection And Biomass Estimation Over Tropical Deciduous Forest. *Geogr. Environ. Sustain. 15, 37–46.* https://doi.org/10.24057/2071-9388-2021-095

Van Zanten, B.T., Brander, L.M., Gutierrez Torres, D., Uyttendaele, G.Y.P., Herrera Garcia, L.D., Patrama, D., Kaczan, D.J., 2021. The Economics of Large-scale Mangrove Conservation and Restoration in Indonesia: Internal Document. World Bank. https://doi.org/10.1596/37605

Zeng, P., Zhang, W., Li, Y., Shi, J., Wang, Z., 2022. Forest Total and Component Above-Ground Biomass (AGB) Estimation through C- and L-band Polarimetric SAR Data. *Forests 13, 442*. https://doi.org/10.3390/f13030442

Zhou, G., Wang, Z., Miao, H., Jiang, C., Jing, G., 2021. Wetland Classification in Poyang Lake Using Dual-polarization Synthetic Aperture Radar Data with Feature Combination. *Sens. Mater. 33, 4607.* https://doi.org/10.18494/SAM.2021.3590

Appendix

Configuration 1 (Dataset with grouping method in median and 25-meter grid size)				
Scenario	MAE	MSE	RMSE	R^2
1	38.76	2435.54	49.35	0.15
2	38.98	2429.21	49.28	0.15
3	43.39	2751.40	52.45	0.04
4	38.56	2398.01	48.97	0.16
5	38.38	2415.25	49.14	0.16
Configuration 2 (Dataset with grouping method in median and 100-meter grid size)				
Scenario	MAE	MSE	RMSE	R^2
1	35.84	2091.00	45.72	0.20
2	36.35	2126.86	46.11	0.19
3	40.49	2459.27	49.59	0.06
4	35.77	2070.99	45.50	0.21
5	35.56	2089.12	45.70	0.20
Configuration 3 (Dataset with grouping method in mean and 25-meter grid size)				
Scenario	MAE	MSE	RMSE	R^2
1	38.92	2399.73	48.98	0.16
2	38.85	2396.90	48.95	0.16
3	43.42	2749.31	52.43	0.04
4	38.49	2385.07	48.83	0.17
5	38.14	2405.57	49.04	0.16
Configuration 4 (Dataset with grouping method in mean and 100-meter grid size)				
Scenario	MAE	MSE	RMSE	R^2
1	35.61	2062.80	45.41	0.21
2	35.61	2092.38	45.74	0.20
3	40.21	2433.96	49.33	0.07
4	35.07	2048.70	45.26	0.22
5	35.47	2060.27	45.39	0.21

Figure A1: The Summarized statistical metrics of the trained models grouped by dataset configuration and parameter usage scenarios.

Figure A2: Mangrove forest prediction maps (in Mg/ha) for each parameter usage scenarios and dataset configuration for model training.